Provided for non-commercial research and education use.
Not for reproduction, distribution or commercial use.

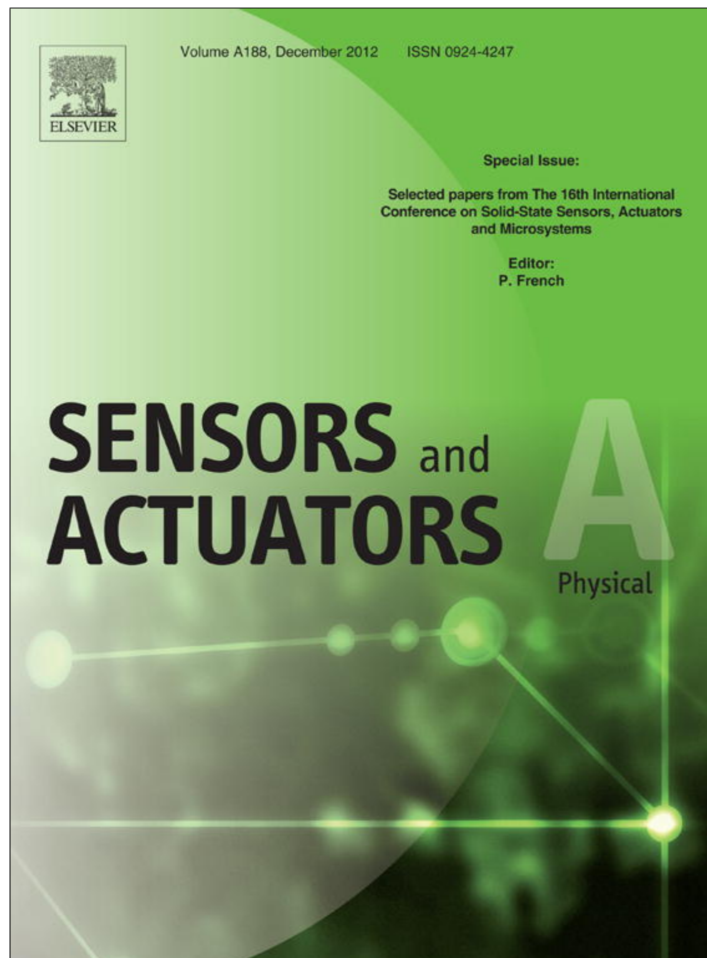

This article appeared in a journal published by Elsevier. The attached copy is furnished to the author for internal non-commercial research and education use, including for instruction at the authors institution and sharing with colleagues.

Other uses, including reproduction and distribution, or selling or licensing copies, or posting to personal, institutional or third party websites are prohibited.

In most cases authors are permitted to post their version of the article (e.g. in Word or Tex form) to their personal website or institutional repository. Authors requiring further information regarding Elsevier's archiving and manuscript policies are encouraged to visit:

http://www.elsevier.com/copyright

Author's personal copy

Sensors and Actuators A 188 (2012) 82–88

Contents lists available at SciVerse ScienceDirect

Sensors and Actuators A: Physical

journal homepage: www.elsevier.com/locate/sna

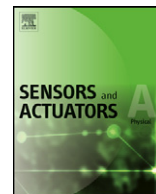

High sensitive dielectric filled Lamé mode mass sensor

Amir Heidari [a,b], Yong-Jin Yoon [b,*], Mi Kyoung Park [a], Woo-Tae Park [c], Julius Ming-Lin Tsai [a,d]

[a] *Institute of Microelectronics, A*STAR (Agency for Science, Technology and Research), Singapore 117685, Singapore*
[b] *Department of Mechanical and Aerospace Engineering, Nanyang Technological University, Singapore 639798, Singapore*
[c] *Department of Mechanical and Automotive Engineering, Seoul National University of Science and Technology, Seoul 139743, Republic of Korea*
[d] *Department of Electrical and Computer Engineering, National University of Singapore, Singapore 117576, Singapore*

ARTICLE INFO

Article history:
Available online 4 April 2012

Keywords:
Mass sensor
Mass sensitivity
Capacitive filled gap transducer
Limit of detection

ABSTRACT

A new high performance mass sensor is designed and fabricated. The mass sensor is a single-crystal silicon squared resonator with dielectric filled capacitive excitation mechanism. The resonators were fabricated using the silicon-on-insulator MEMS process. In order to study the mass sensitivity of the fabricated resonator, a polyelectrolyte multilayer (PEM) is used to coat on the resonator surface. The resonator has the resonance frequency of 34.81 MHz, mass sensitivity of 105.4 μm^2/ng. Experimental measurements of the mass sensitivities agree with theoretical predictions. The new developed mass sensor shows a high potential to be used in gas sensing and bio detection applications.

© 2012 Elsevier B.V. All rights reserved.

1. Introduction

In many biological applications, high performance mass sensors are required to capture small biological entities (e.g. low concentrated solution). Advances in micro- and nanofabrication technologies are enabling a wide range of new technologies, including the development of acoustic wave resonators with high potential for very high mass sensitivity [1–3]. However, further miniaturization of mass sensors using nanofabrication techniques suffer from the low device-to-device performance reproducibility and difficulties to interface to measurement equipments [4].

The quartz crystal microbalance (QCM) is the best example of resonant mass sensor that has been commercialized for film thickness monitoring and other mass sensing applications [5,6]. However, despite the extensive use of QCM technology, their application is limited with the high cost due to their complex manufacturing and the difficulties in applying them for sensor arrays due to lack of integration capability and appropriate characterization interface.

Application of the air-gap Lamé mode resonator has been widely studied in communication applications [7,8], but few researchers have demonstrated this resonator type for mass sensing application [9,10]. In this work, we have developed a high sensitivity mass sensor using a single-crystal silicon squared resonator. The resonator is excited using capacitive excitation in the Lamé bulk acoustic resonant mode at a frequency of 34.81 MHz. The transducer capacitive gap is filled with silicon nitride which helps to achieve smaller gap and as a result much higher electrostatic force in comparison with air gap counterparts [11]. Compared to previously reported mass sensors [12–14], the presented sensor shows a potential to detect smaller masses due to its high mass sensitivity. The high mass sensitivity arises from miniaturization of the resonator which leads to an increase in the relative frequency shift for a given amount of adsorbed mass. This high mass sensitivity may be affected by many factors in liquid in bio sensing application, but it gives a good estimation of the mass sensitivity of the sensor in the air for gas sensing application. Furthermore, smaller motional resistance (Rx) is achieved at similar frequencies and bias conditions with air-gap counterpart. This degree of motional resistance reduction comes via not only the higher dielectric constant provided by a nitride-filled electrode-to-resonator gap, but also by the ability to achieve smaller solid gaps than air gaps.

We initially introduced the sensor structure in [15], where the working principal of the resonator, fabrication method and resonance frequency and mass sensitivity simulations are described in detail. The differential drive-and-sense measurement setup and preliminary experimental results are presented in [16,17]. The current paper includes the thorough characterization of the sensor for mass sensing application using a layer-by-layer polymer deposition and comparison of the results with the simulation.

2. Sensor structure and operation

The microresonator consists of a square silicon plate supported by four beams attached to it from the corners (see Fig. 1(a)). The square plate is separated from the surrounding electrodes with a 80 nm nitride gap that defines the capacitance of the electro-mechanical transducer. The resonator is laterally driven

* Corresponding author. Tel.: +65 6790 5033.
E-mail address: YONGJINY@ntu.edu.sg (Y.-J. Yoon).

0924-4247/$ – see front matter © 2012 Elsevier B.V. All rights reserved.
http://dx.doi.org/10.1016/j.sna.2012.03.040

Author's personal copy

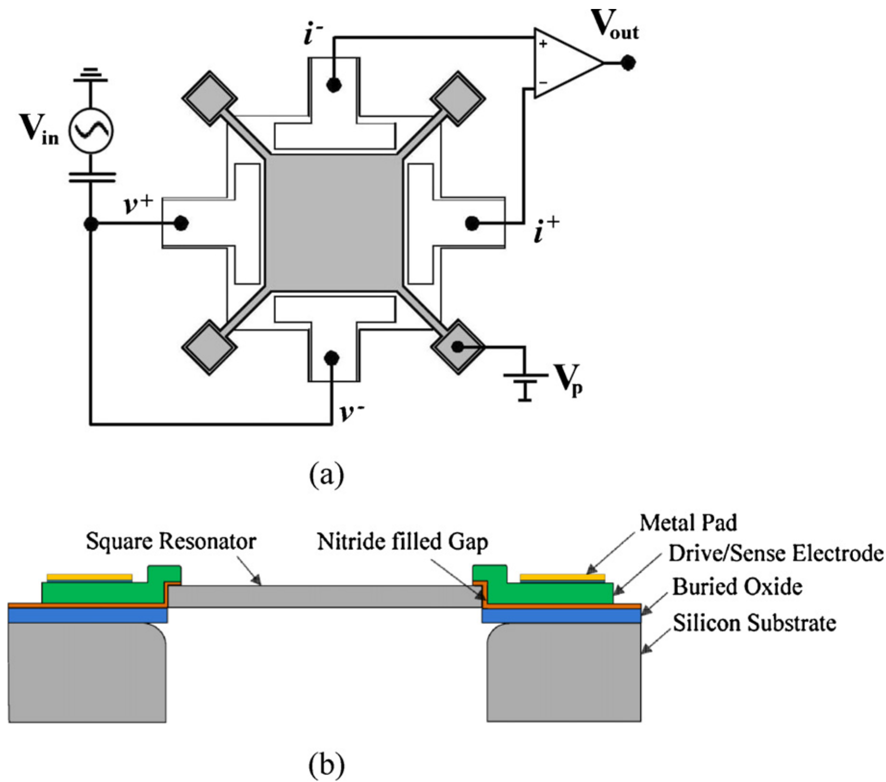

Fig. 1. (a) Schematic of the device showing the resonator, exciting and sensing electrodes, driving and biasing setup. (b) Cross-sectional view of the square resonator, depicting the 80 nm solid gap between resonator and its electrodes.

with electrodes on two opposite sides of the square plate symmetrically. A DC-bias voltage (V_p) is applied to the structure via the anchors, while two AC input voltages are applied to the input electrodes with 180° of phase difference. These voltages result in a time-varying electrostatic force on the plate edges which makes it oscillate in its fundamental frequencies in the Lamé mode. The capacitive gap distances of the opposite side change with this frequency. Because of the electrostatic field in the gap, a time-varying current is induced in the output electrode. A cross-sectional view of the square resonator, showing the nitride gap between resonator and its electrodes is depicted in Fig. 1(b). The filled nitride gap defines the capacitive gap of the input and output capacitors.

The square resonator is simulated using COMSOL Multiphysics and the Lamé mode is shown in Fig. 2. In this mode, adjacent edges of the square plate bend in anti-phase while the plate volume is preserved. Nodal points of resonance are located at the four corners of the square and at the centre of the plate.

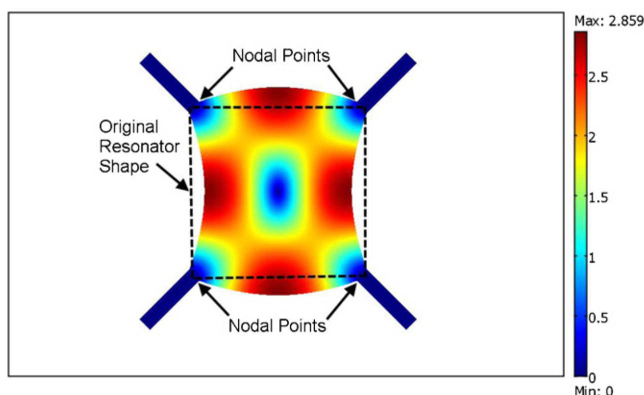

Fig. 2. FEM simulation of square resonator with side length of 100 μm in Lamé mode in COMSOL-Multiphysics software. (The simulated resonant frequency is 38.74 MHz.)

If the material of the square plate is homogeneous and isotropic, and if the side length of square, L is much larger than its thickness, the square resonator can be theoretically modelled as a thin plate. In this case, the resonant frequency of Lamé mode can be calculated as below [18]:

$$f_0 = \frac{n}{\sqrt{2}L}\sqrt{\frac{C_{44}}{\rho}} \quad (1)$$

where n is the order of the resonance mode, ρ is the material density and C_{44} is stiffness constant which can be replaced by shear modulus term G. For the single-crystal silicon structure, the material properties are as follows: $\rho = 2330\,\mathrm{kg/m^3}$ and $G = 70$ GP. Replacing these values in Eq. (1), the corresponding resonant frequency of a square resonator with $L = 100\,\mu\mathrm{m}$ will be $f_0 = 38.75$ MHz.

3. Derivation of mass sensitivity

The capacitive square resonator presented here actually worked as a mass sensor. The working principle of this sensor is that the resonant frequency of the resonator decreases in response to a mass loading on its surface. Mass sensitivity is defined as the shift in the sensor resonance frequency due to the changes in the mass. A higher mass sensitivity helps to measure smaller masses. The mass sensitivity S_m of the bulk-wave resonator mass sensor is defined by Sauerbrey equation as below [19]:

$$S_m = -\lim_{\Delta m \to 0} \frac{1}{f_0}\frac{\Delta f}{\Delta m} \quad (2)$$

where Δm is the external added mass on the surface per unit area of the sensor, due to absorption or thin film deposition and $\Delta f = f - f_0$ is the frequency shift in response to the mass loading. The negative sign in Eq. (2) is to be cancelled out with frequency change (Δf)

Author's personal copy

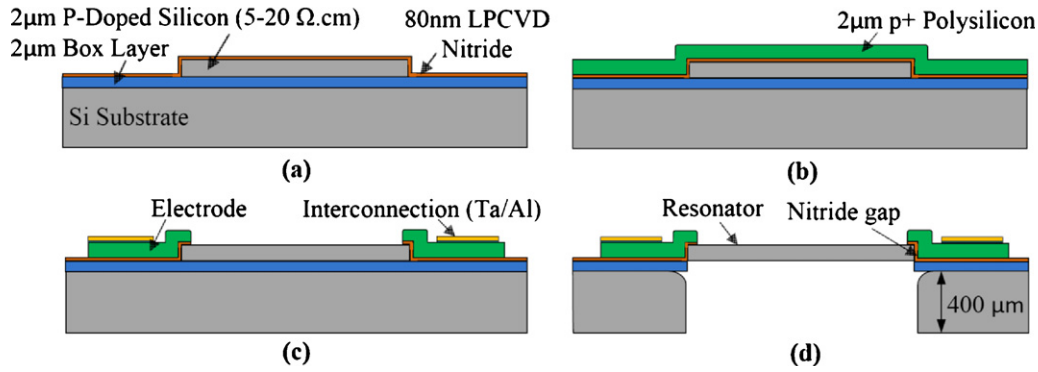

Fig. 3. Fabrication process flow. (a) Pattern and etching the resonator and its anchors on the SOI wafer and deposition 80 nm thick LPCVD nitride. (b) Deposition of 2 μm polysilicon and doping with boron to get p+ polysilicon. (c) Pattern and etching the poly to define the electrodes and doing the metallization on electrodes. (d) Backside etch using DRIE to release the resonator backside.

since the resonance frequency decreases after adding the mass on the resonator surface. Eq. (1), can be modified based on the mass per unit area (m) of the resonator as $m = \rho t$;

$$f_0 = \frac{n}{\sqrt{2}L}\sqrt{\frac{C_{44}t}{m}} \tag{3}$$

where t is the resonator thickness. Taking the derivative of Eq. (3) with respect to m, and using this definition again, we obtain:

$$\frac{df}{dm} = -\frac{1}{2m}\cdot\frac{n}{\sqrt{2}L}\sqrt{\frac{C_{44}t}{m}} = -\frac{f_0}{2m} \tag{4}$$

As a result, Eq. (2) can be rewritten as below:

$$S_m = \frac{1}{2m} = \frac{1}{2\rho t} \tag{5}$$

The definition of the mass sensitivity is not dependant to the lateral dimension, the amount of deposited mass and the material properties of deposited layer and only depends on the density of the resonator structure material (ρ) and resonator's thickness (t). As a result, a sensor with a thinner structure can have a higher mass sensitivity. It should be considered that Eq. (5) is only valid when the resonator is vibrating in the air or vacuum. In the liquid environment, the resonators performance is affected with many other factors. As the energy loss arises from viscous damping of liquid, the mass sensitivity of the resonator cannot be specified with this equation. In addition, Eq. (5) is valid when the mass is strongly bound (non slip boundary condition) to the surface of the resonator.

The mass sensitivity value (S_m) of the fabricated devices was analytically evaluated for the air environment and found to be 107.29 μm^2/ng for a 38.75 MHz resonator (L = 100 μm, t = 2 μm, ρ = 2330 kg/m^3). This value is calculated considering that the sensitive layer is uniformly spread over the entire top surface of the resonator. It is quite a challenge to generate a sensor coated with 100% uniform biomolecules in practice. However, this fact does not influence on the resonance frequency, resonance mode and actual mass sensitivity of the sensor. A 3D Finite Element Method (FEM) analysis has been performed with the aid of COMSOL Multiphysics to validate the obtained analytical values of mass sensitivity (S_m). A thin square-shaped mass was added to the surface of the resonator. Then, the device sensitivity was evaluated by gradually varying the density of the added mass and computing the corresponding linear shift in the resonance frequency. The simulated value of the mass sensitivity is obtained to be 107.34 μm^2/ng, which shows a good agreement between analytical and simulated values.

The sensor resolution is restricted with environment and measurement noises which are characterized with limit of detection (LOD). LOD describes the smallest amount of mass that a sensor can detect considering the existing noises. Lower value of LOD means that smaller mass can be detected. The LOD of acoustic mass sensor is given by [20]

$$\text{LOD} = \frac{N}{S_m \cdot f_0} \tag{6}$$

where N is the noise level of the sensor and is equal to 3 times of the standard deviation of measured resonance frequency of a bare resonator ($N = 3\sigma$) and S_m is the mass sensitivity defined in Eq. (2). LOD discussed above is given in terms of detectable mass per unit area.

4. Fabrication process

The fabrication starts with a Silicon on Insulator (p-type SOI wafer). The thickness of device layer in the SOI wafer is 2 μm. The fabrication follows with patterning the resonator and its anchors on the SOI wafer and deposition 80 nm thick LPCVD nitride. Then, a layer of 2 μm LPCVD polysilicon is deposited to have the required layer for electrodes. The deposited polysilicon is implanted (boron, doses = 2E15 cm^{-2}, energy = 180 keV, tilt = 7°) and annealed (N_2, 1 h, 950 °C). The polysilicon layer is then patterned and etched to define the resonator surrounding electrodes. Then interconnections are formed by deposition, patterning and etching 500 Å and 7500 Å of tantalum (for adhesion purpose) and aluminum, respectively. To release the backside of resonator, a DRIE etch is used. The fabrication process flow is summarized in Fig. 3.

Filling the capacitive gap with silicon nitride helps to achieve smaller gap distance in comparison with air gap counterparts [11]. Filling the gap also provides some other benefits since it better stabilizes the resonator structure against shock and eliminates the possibility of particles or liquid getting into the electrode-to-resonator air gap, which poses a potential reliability issue. Fig. 4 presents the SEM image of a fabricated micromechanical Lamé mode resonator, together with a cross section image of the resonator, nitride gap and its surrounding polysilicon electrode (obtained from transmission electron microscope (TEM)).

5. Sensor characterization

In order to characterize the fabricated resonator, its surface area should be coated with a uniform and non-slip mass. In this work, Polyelectrolyte Multilayer (PEM) is used for these purposes [21,22]. After coating of each PEM layer (a specified amount of mass), a new frequency measurement is required. The required steps for the PEM coating and sensor characterization are explained in below sub sections.

Author's personal copy

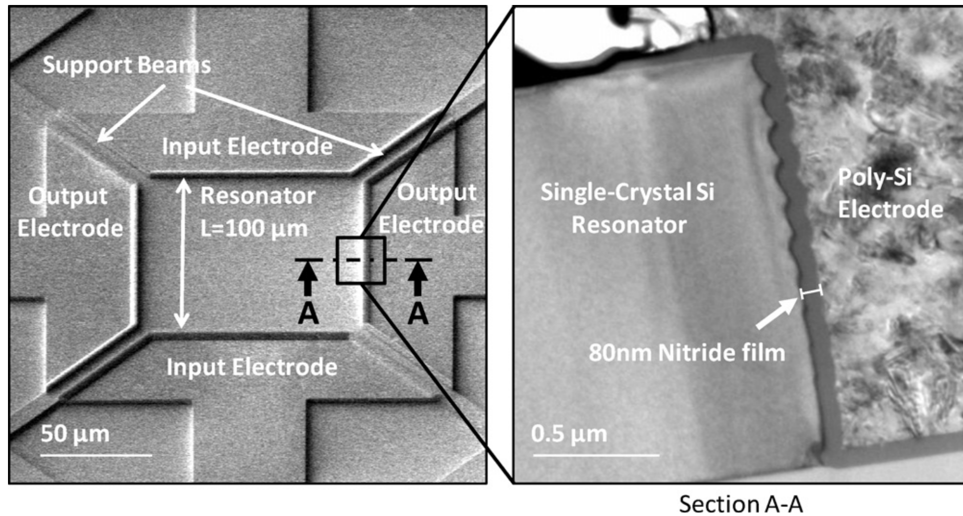

Fig. 4. SEM image of the fabricated mass sensor and TEM image of the cross-section of Si resonator, nitride gap and its surrounding polysilicon electrode.

5.1. Polyelectrolyte multilayer coating

PEM is in fact a polymer forms by the sequential deposition of two oppositely charged polyelectrolytes (poly sodium 4-styrensulfonate (PSS) and polyallylamine hydrochloride (PAH)). They have the ability of self-assembling on the surface in a controlled layer-by-layer fashion. PAH is a positive charge polymer and PSS has the negative charge.

As PEM can only be coated on the charged surfaces, the silicon resonator surface has to be functionalized beforehand. In this work, a 2% solution of 3-aminopropyltriethoxysilane (APTES) is used for 2 h to charge the silicon resonator surface. APTES is a highly effective silane coupling agent that is used on silicon and some other substrates to enhance the adhesion [22]. As the APTES make a positive charged layer on silicon surface, the coating process starts with the negatively charged polymer (PSS) and followed by the positive charged polymer (PAH). Polymer films are built by alternately dipping the chip in aqueous solutions of PAH (1 mg/mL) and PSS (1 mg/mL) for 15 min each. After each polymer adsorption, the chip is rinsed two times in deionized (DI) water with the assist of shaker table for 5 min. PEM is formed by successive dipping in aqueous PSS and PAH solutions. The required steps for polymer coating on silicon surface are summarized in Fig. 5.

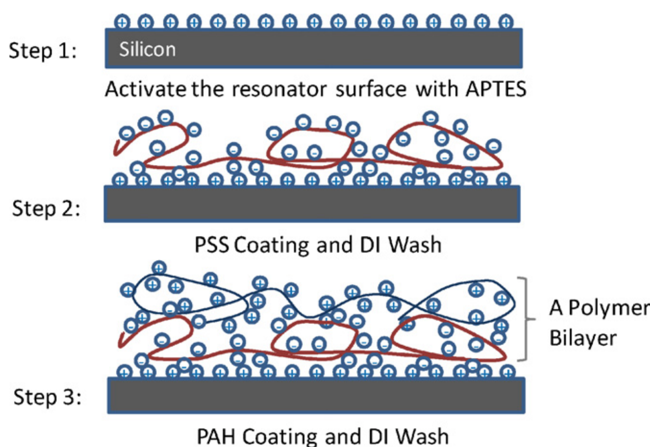

Fig. 5. Coating steps of PEM: (1) activate the resonator surface with APTES; (2) dipping in PSS solution and rinsing in DI water; (3) dipping in PAH solution and rinsing in DI water.

A PAH and PSS layers together referred as one bilayer. Thickness of each polymer bilayer is a function of sodium chloride concentration used in polymer solution preparation. In a 50 mL of PEM solution, we used 50 mM of sodium chloride. Having this concentration, the theoretical thickness of one bilayer of PAH/PSS is ~1.7 nm [23]. In order to verify the real thickness of coated polymer, samples are prepared by Focused Ion Beam (FIB), and the thicknesses are measured from TEM images. After coating of 12 bilayers of PEM, the measured thickness of the PEM is 19.5 nm which is in a good agreement with the 20.4 nm of theoretical thickness of 12 bilayers. Having the thickness of each polymer bilayer and the density of 1340 kg/m^3 of the PEM [24], the amount of coated mass per unit area, Δm on resonators can be estimated.

5.2. Measurement setup

We used the Agilent 4395A network analyzer to test the fabricated sensors. This network analyzer is used to apply the AC voltage to the sensor and measure the output signal. Fig. 6 shows the fully differential drive-and-sense measurement setup implemented in this work. The electrical elements are placed on a printed circuit board (PCB).

The AC drive signal is split into positive and negative signals through a single-to-differential conversion block. The polarization DC voltage, V_p is combined with AC voltage and applied to the resonator. The resonator die is wire bonded to the PCB. The SOI substrate is grounded to reduce the parasitics caused by feed through capacitance. The resonator's output current is sensed using a differential transresistance amplifier setup. Finally, the magnitude and phase of the transmission coefficient, S21 is measured with the network analyzer. The setup is shown in Fig. 1(a) is simpler alternative to a fully differential sensing method.

5.3. Experimental results and discussion

The initial measurements are performed for bare resonators, to get the resonance frequency and the *Q*-factor. S21 parameter is measured for a $L = 100\,\mu$m resonator and the transmission and phase are depicted in Fig. 7. The resonance frequency of this resonator is measured at 34.81 MHz with a Q value of 1800 in an atmospheric pressure when the resonator is biased with a DC voltage of 20 V and an AC drive voltage of 0.63 Vpp.

The difference between the theoretical frequency (38.75 MHz) and the measured frequency (34.81 MHz) can be related to the

Author's personal copy

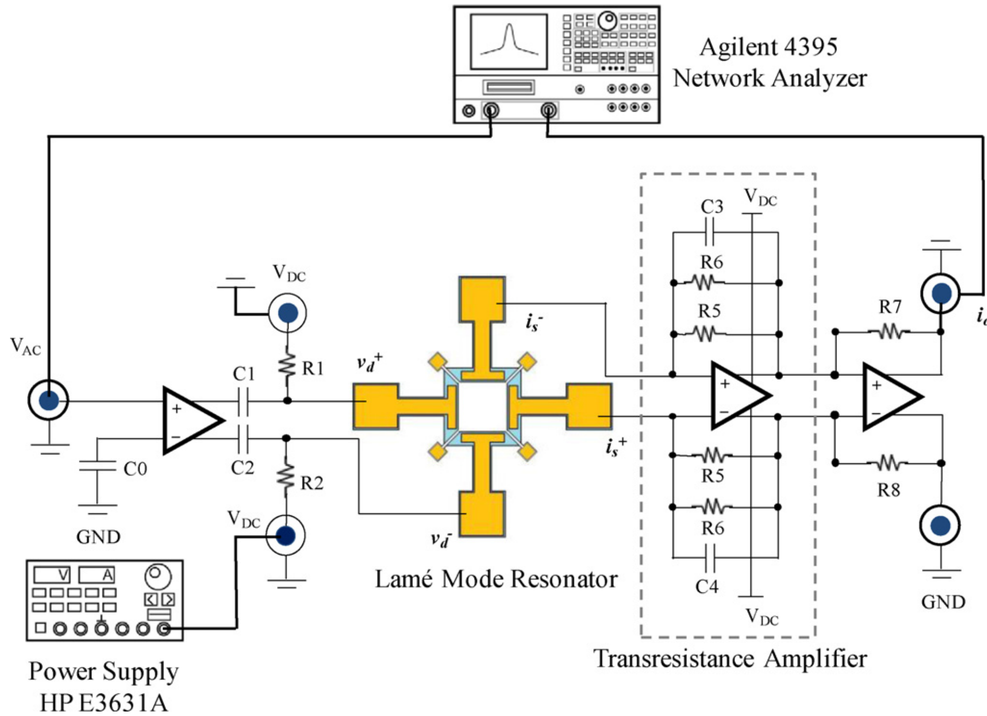

Fig. 6. Differential drive-and-sense measurement setup.

difference in the Young's modulus used in the simulation (E = 169 GPa) and as its real value.

Before coating, the resonance frequency of non-coated resonators (after functionalizing their surface with APTES) is measured and considered as the reference frequency (f_0) for all later frequency shift calculations ($\Delta f_{(i)} = f_{(i)} - f_0$). The notation $f_{(i)}$ refers to the resonance frequency of the sensor after coating of i-th polymer bilayer (i = 4, 6,. . .,12). The chips were stored in nitrogen box for a few hours to be dried after each polymer coating step. The polyelectrolyte coating is known to be not uniform up to 4 bilayers [25]. As a result, the frequency shift would not be linear below 4 bilayers and thus we measured the first frequency shift after coating of 4 bilayers. Thin polymer film successfully formed by the successive deposition of PAH and PSS up to 12 bilayers on the resonators surface. Five frequencies are recorded for each measurement after every 2 bilayers coating to calculate the error bar. Fig. 8 shows the measured frequency shifts ($\Delta f_{(i)}$) of 34.81 MHz resonator versus the number of polymer coated bilayers and their corresponding masses. It can be seen that the frequency shift is linearly correlated with the number of coated polymer bilayers for all resonators.

The mass sensitivity of the resonator can be calculated now from the measured frequency shifts and Eq. (2). In order to obtain the limit of detection (LOD) of sensors, the standard deviation of the resonance frequency of each resonator is measured. For this

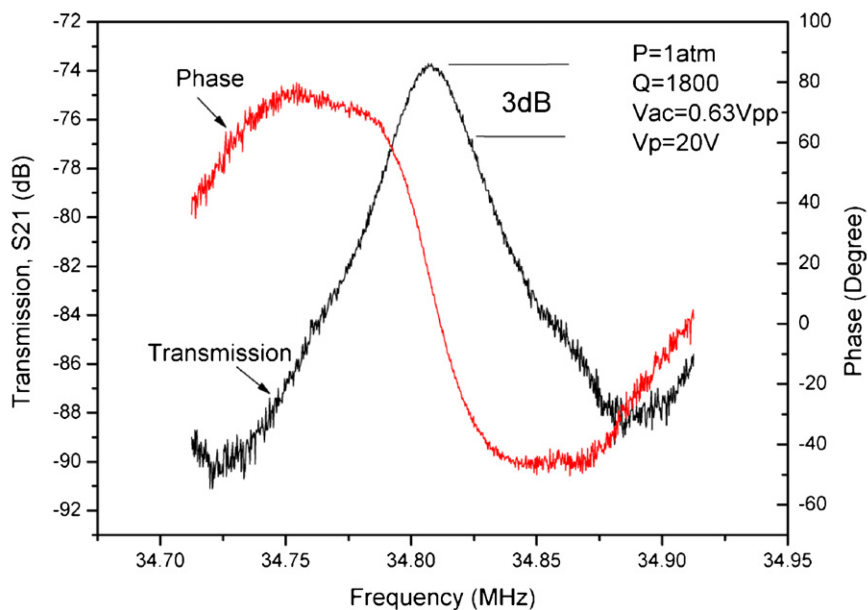

Fig. 7. Measured transmission (magnitude and phase curves) of 34.81 MHz Lamé-mode square at atmospheric pressure and bias voltage of 20 V DC, 0.63 Vpp AC and measured Q of 1800.

Author's personal copy

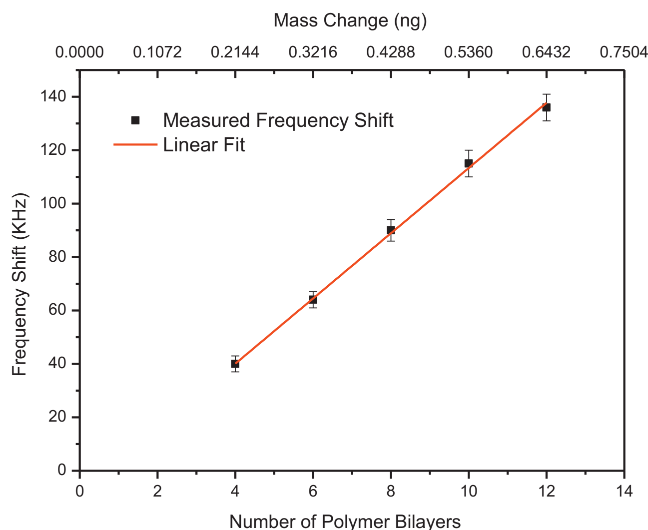

Fig. 8. Absolute frequency shift, $|\Delta f_{(i)}|$ versus number of coated PEM bilayers and its corresponding mass change for the 34.81 MHz resonator.

Table 1
Measured resonance frequency, mass sensitivity, noise, LOD of three fabricated sensors.

Frequency, f_0 (MHz)	Mass sensitivity, S_m (μm^2/ng)	Noise, 3σ (kHz)	LOD ($\times 10^{-6}$ ng/μm^2)
34.81 ($L = 100\,\mu m$)	104.23	4.95	1.36
30.1 ($L = 120\,\mu m$)	106.31	6.24	1.95
24.2 ($L = 150\,\mu m$)	105.62	6.83	2.67

purpose, the number of 30 data points ($n = 30$) are recorded for each sensor with the rate of 1 sample/min. Frequency shift measurements are repeated for two more resonators with different lateral size and their measured resonance frequency, mass sensitivity and limit of detection are listed in Table 1.

It can be seen from the Table 1 that the mass sensitivity is independent from the lateral size (L) of resonators as it expected from Eq. (5). The average S_m is 105.4 μm^2/ng, which coincides with the theoretical mass sensitivity (107.29 μm^2/ng). This amount of mass sensitivity is not the best reported mass sensitivity in the literature, but still is higher than some of reported mass sensors like QCM [13,26] and magnetoelastic [14] sensors with mass sensitivities of 1.13 μm^2/ng and 36.19 μm^2/ng, respectively. The obtained mass sensitivity is also much higher than the piezoelectric membrane-based biosensor [27] with mass sensitivity of 16.5 μm^2/ng. The main reason of this high mass sensitivity of the developed sensor in comparison with these sensors is its relative thin resonator structure (2 μm). Again, it should be considered that the obtained mass sensitivity is only valid when the resonator is vibrating in the air or vacuum (for application like gas sensing). In the liquid environment (for application like bio sensing), the resonators performance is affected with many other factors and the obtained mass sensitivity may be very different.

As the experiments are performed in the normal environment condition, the obtained limit of detection (LOD) includes the unwanted ambient noise (temperature variations) and also measurement equipments' noises (imperfect electrical connections) which are all considered as our measurement limitations. As a result, the obtained LOD is rather high comparing the state of the art sensors like FBAR ($\sim 10^{-8}$ ng/μm^2) [28]. We are currently working on optimizing the characterizations of the electronic interface to reduce the noises and improve the LOD of the developed sensor in future work.

6. Conclusion

In conclusion, a silicon Lamé mode bulk acoustic resonator has been demonstrated for the use in mass sensing application (gas sensing). Mass sensitivity of 105.4 μm^2/ng and limit of detection of 1.36×10^{-6} ng/μm^2 have been measured. The high mass sensitivity arises from miniaturization of the resonator (2 μm thick resonator) which leads to an increase in the relative frequency shift for a given amount of adsorbed mass. In addition, the compact size of the resonator helps that a small sample volume to be required in real bio applications. The demonstration of the sensor characterizations makes this new technology suitable for the fabrication of compact, low cost and high performance biosensors platform for mass detection.

References

[1] D. Grieshaber, R. MacKenzie, J. Vörös, E. Reimhult, Electrochemical biosensors-sensor principles and architectures, Journal of Sensors 8 (2008) 1400–1458.
[2] R. Bashir, BioMEMS: state-of-the-art in detection, opportunities and prospects, Advanced Drug Delivery Reviews 56 (2004) 1565–1586.
[3] J.L. Arlett, E.B. Myers, M.L. Roukes, Comparative advantages of mechanical biosensors, Nature Nanotechnology 6 (2011) 203–215.
[4] Y.T. Yang, C. Callegari, X.L. Feng, K.L. Ekinci, M.L. Roukes, Zeptogram-scale nanomechanical mass sensing, Nano Letters 6 (2006) 583–586.
[5] L. Rodriguez-Pardo, J.F. Rodriguez, C. Gabrielli, H. Perrot, R. Brendel, Sensitivity, noise, and resolution in QCM sensors in liquid media, Journal of Sensors IEEE 5 (2005) 1251–1257.
[6] V. Heitmann, B. Reiß, J. Wegener, in: O.S. Wolfbeis (Ed.), The Quartz Crystal Microbalance in Cell Biology: Basics and Applications, Springer Ser Chem Sens Biosens, 2007, pp. 303–338.
[7] S.A. Bhave, G. Di, R. Maboudian, R.T. Howe, Fully-differential poly-SiC lame mode resonator and checkerboard filter, in: 18th IEEE International Conference on Micro Electro Mechanical Systems, 2005, pp. 223–226.
[8] L. Khine, M. Palaniapan, High-Q bulk-mode SOI square resonators with straight-beam anchors, Journal of Micromechanics and Microengineering 19 (1) (2009) 015017.
[9] J.E.Y. Lee, B. Bahreyni, Y. Zhu, A.A. Seshia, Ultrasensitive mass balance based on a bulk acoustic mode single-crystal silicon resonator, Journal of Applied Physics and Letters 91 (2007).
[10] A.T.H. Lin, J. Yan, A.A. Seshia, Mechanically coupled bulk-mode dual resonator mass sensor, Procediga Engineering 5 (2010) 1454–1457.
[11] J.R. Clark, W.T. Hsu, M.A. Abdelmoneum, C.T.C. Nguyen, High-Q UHF micromechanical radial-contour mode disk resonators, Journal of Microelectronic Systems 14 (2005) 1298–1310.
[12] A. Janshoff, H.-J. Galla, C. Steinem, Piezoelectric mass-sensing devices as biosensors—an alternative to optical biosensors? Angewandte Chemie 39 (2000) 4004–4032.
[13] M. Nirschl, M. Schreiter, J. Vörös, Comparison of FBAR and QCM-D sensitivity dependence on adlayer thickness and viscosity, Journal of Sensors and Actuators A: Physical 165 (2011) 415–421.
[14] W. Shen, L.C. Mathison, V.A. Petrenko, B.A. Chin, Design and characterization of a magnetoelastic sensor for the detection of biological agents, Journal of Physics D: Applied Physics 43 (2010) 015004.
[15] A. Heidari, Y.-J. Yoon, M.-K. Park, W.-T. Park, J. Tsai Ming Lin, Developing high sensitivity biomass sensor using lamé mode square resonator, Advanced Materials Research 254 (46) (2011) 46–49.
[16] A. Heidari, Y.-J. Yoon, M.-K. Park, W.-T. Park, J. Tsai Ming Lin, Ultrasensitive dielectric filled Lamé mode biomass sensor, in: Transducers' 11, Beijing, China, 2011.
[17] A. Heidari, Y.-J. Yoon, M.-K. Park, W.-T. Park, J. Tsai Ming Lin, Design and simulation of a dielectric field capacitive transducer, in: International Conference of Micro- and Nano-Engineering (MNE), Berlin, Germany, 2011.
[18] S. Basrour, H. Majjad, J.-R. Coudevylle, M. de Labachelerie, in: B. Courtois, J.M. Karam, S.P. Levitan, K.W. Markus, A.A.O. Tay, J.A. Walker (Eds.), Design and test of new high-Q microresonators fabricated by UV-LIGA, SPIE, Cannes-Mandelieu, France, 2001, pp. 310–316.
[19] S.W. Wenzel, R.M. White, Analytic comparison of the sensitivities of bulk-wave, surface-wave, and flexural plate-wave ultrasonic gravimetric sensors, Journal of Applied Physics and Letters 54 (1989) 1976–1978.
[20] D. Lange, C. Hagleitner, A. Hierlemann, O. Brand, H. Baltes, Complementary metal oxide semiconductor cantilever arrays on a single chip: mass-sensitive detection of volatile organic compounds, Journal of Analytical Chemistry 74 (2002) 3084–3095.
[21] J.M. Lourenço, P.A. Ribeiro, A.M. Botelho do Rego, F.M. Braz Fernandes, A.M. Moutinho, M. Raposo, Counterions in poly(allylamine hydrochloride) and poly(styrene sulfonate) layer-by-layer films, Langmuir 20 (2004) 8103–8109.

Author's personal copy

[22] J. Dai, D.M. Sullivan, M.L. Bruening, Ultrathin, layered polyamide and polyimide coatings on aluminum, Industrial & Engineering Chemistry Research 39 (2000) 3528–3535.
[23] J. Kim, J. Cho, P.M. Seidler, N.E. Kurland, V.K. Yadavalli, Investigations of chemical modifications of amino-terminated organic films on silicon substrates and controlled protein immobilization, Langmuir 26 (2010) 2599–2608.
[24] Z. Feldötö, I. Varga, E. Blomberg, Influence of salt and rinsing protocol on the structure of PAH/PSS polyelectrolyte multilayers, Langmuir 26 (2010) 17048–17057.
[25] F. Caruso, K. Niikura, D.N. Furlong, Y. Okahata, Ultrathin multilayer polyelectrolyte films on gold: construction and thickness determination, Langmuir 13 (1997) 3422–3426.
[26] K.A. Marx, Quartz crystal microbalance: a useful tool for studying thin polymer films and complex biomolecular systems at the solution—surface interface, Biomacromolecules 4 (2003) 1099–1120.
[27] T. Xu, Z. Wang, J. Miao, L. Yu, C.M. Li, Micro-machined piezoelectric membrane-based immunosensor array, Journal of Biosensors and Bioelectronics 24 (2008) 638–643.
[28] M. Nirschl, A. Blüher, C. Erler, B. Katzschner, I. Vikholm-Lundin, S. Auer, J. Vörös, W. Pompe, M. Schreiter, M. Mertig, Film bulk acoustic resonators for DNA and protein detection and investigation of in vitro bacterial S-layer formation, Sensors and Actuators A: Physical 156 (1) (2009) 180–184.

Biographies

Amir Heidari received his B.Sc. and M.Sc. degrees in Mechanical Engineering from Bu Ali Sina University (BASU) and Iran University of Science and Technology (IUST), Tehran, Iran in 2003 and 2005, respectively. He is currently a Ph.D. student in Nanyang Technological University, Singapore and attached student to Institute of Microelectronics (IME). His research interest is in the design and fabrication of MEMS sensors.

Yong-Jin Yoon joined Department of Mechanical and Aerospace Engineering at Nanyang Technological University (NTU) as an Assistant Professor in January, 2010. He obtained his Ph.D. degree in the Mechanical Engineering at Stanford University in September 2009. During his PhD study, he also obtained two Master degrees in Stanford: one in Electrical Engineering, focusing on MEMS and Signal Processing, and the other in Mechanical Engineering, focusing on Medical Device Design. Currently, his researches at NTU include biomimetic electroacoustic MEMS transducer, bio-chemical MEMS sensor, and medical device.

Mi Kyoung Park received the B.S. and M.S. degrees in chemical engineering from Hong-Ik University, Seoul, Korea, in 1996 and 1998, respectively, and the Ph.D. degree in chemistry from Department of Chemistry, University of Houston, Houston, TX in 2003. She is currently a Scientist II in the Bio-Electronics Programme, Institute of Microelectronics, Agency for Science, Technology and Research (A*STAR), Singapore. Her main research areas are label-free immunosensors such as FET sensor, SPR sensor, silicon photonics sensor, and electrochemical sensor for biomedical applications and surface chemistry for surface modification and biomolecule immobilization.

Woo-Tae Park received the B.S. degree in mechanical design from Sungkyunkwan University, Korea, in 2000, the M.S. and Ph.D. degrees in mechanical engineering from Stanford University in 2002 and 2006 respectively. For his Ph.D., he worked on wafer scale encapsulated MEMS devices for biomedical applications. After graduation, he worked at Intel Corporation, and then went to Freescale Semiconductor, leading several projects on MEMS development. He has authored more than 52 journals and refereed conference papers and has 14 issued and pending patents. He is currently the Project Leader at IME for implantable biomedical MEMS sensors systems and wireless neural probes.

Julius Ming-Lin Tsai received the B.S. and Ph.D. degrees in power mechanical engineering from National Tsing Hua University, Hsin-Chu, Taiwan, in 1995 and 2004, respectively. From 2004 to 2009 he joined VIA Technologies, where he was involved with high-frequency small-signal modeling. He is now a principle investigator in Institute of Microelectronics, Singapore and an adjunct assistant professor with Department of Electrical and Computer Engineering, National University of Singapore. His main research interests are in RFMEMS, NEMS switch and MEMS ultrasound transducers. Dr. Tsai was the recipient of a scholarship presented by the National Science Council of Taiwan.